

Lethal myelofibrosis induced by *Bmi1*-deficient hematopoietic cells unveils a tumor suppressor function of the polycomb group genes

Hideyuki Oguro,^{1,6} Jin Yuan,^{1,6} Satomi Tanaka,^{1,2} Satoru Miyagi,^{1,6} Makiko Mochizuki-Kashio,^{1,6} Hitoshi Ichikawa,³ Satoshi Yamazaki,^{4,7} Haruhiko Koseki,⁵ Hiromitsu Nakauchi,^{4,7} and Atsushi Iwama^{1,6}

¹Department of Cellular and Molecular Medicine, Graduate School of Medicine, Chiba University, Chiba 260-8670, Japan

²Department of Hematology, Chiba University Hospital, Chiba 260-8670, Japan

³Division of Genetics, National Cancer Center Research Institute, Tokyo 104-0045, Japan

⁴Division of Stem Cell Therapy, Center for Stem Cell Biology and Regenerative Medicine, Institute of Medical Science, University of Tokyo, Tokyo 108-8639, Japan

⁵Laboratory for Lymphocyte Development, RIKEN Research Center for Allergy and Immunology, Yokohama 230-0045, Japan

⁶Japan Science and Technology Agency (JST), Core Research for Evolutional Science and Technology and ⁷ERATO, Gobancho, Chiyoda-ku, Tokyo 102-0076, Japan

Polycomb-group (PcG) proteins form the multiprotein polycomb repressive complexes (PRC 1 and 2, and function as transcriptional repressors through histone modifications. They maintain the proliferative capacity of hematopoietic stem and progenitor cells by repressing the transcription of tumor suppressor genes, namely *Ink4a* and *Arf*, and thus have been characterized as oncogenes. However, the identification of inactivating mutations in the PcG gene, *EZH2*, unveiled a tumor suppressor function in myeloid malignancies, including primary myelofibrosis (PMF). Here, we show that loss of another PcG gene, *Bmi1*, causes pathological hematopoiesis similar to PMF. In a mouse model, loss of *Bmi1* in *Ink4a-Arf*^{-/-} hematopoietic cells induced abnormal megakaryocytopoiesis accompanied by marked extramedullary hematopoiesis, which eventually resulted in lethal myelofibrosis. Absence of *Bmi1* caused derepression of a cohort of genes, including *Hmga2*, which is an oncogene overexpressed in PMF. Chromatin immunoprecipitation assays revealed that *Bmi1* directly represses the transcription of *Hmga2*. Overexpression of *Hmga2* in hematopoietic stem cells induced a myeloproliferative state with enhanced megakaryocytopoiesis in mice, implicating *Hmga2* in the development of pathological hematopoiesis in the absence of *Bmi1*. Our findings provide the first genetic evidence of a tumor suppressor function of *Bmi1* and uncover the role of PcG proteins in restricting growth by silencing oncogenes.

CORRESPONDENCE

Atsushi Iwama:
aiwama@faculty.chiba-u.jp

Abbreviations used: CFC, colony-forming cell; ChIP, chromatin immunoprecipitation; CLP, common lymphoid progenitor; CMP, common myeloid progenitor; GMP, granulocyte/macrophage progenitor; H2Aub1, mono-ubiquitination of histone H2A; HPP-CFC, high proliferative potential-CFC; HSC, hematopoietic stem cell; LMPP, lymphoid-primed MPP; LSC, leukemic stem cell; LSK, Lineage⁻Sca-1⁺c-Kit⁺; MEP, megakaryocyte/erythroid progenitor; MPN, myeloproliferative neoplasm; MPP, multipotent progenitor; PcG, polycomb-group; PMF, primary myelofibrosis; PRC, polycomb repressive complex.

Polycomb-group (PcG) proteins are transcriptional repressors that function in gene silencing by modulating chromatin structure. They form the chromatin-associated multiprotein complexes, polycomb repressive complex (PRC) 1 and PRC2 (Simon and Kingston, 2009). PcG proteins have been implicated in the maintenance of self-renewing stem cells (Pietersen and van Lohuizen, 2008; Konuma et al., 2010; Sauvageau and Sauvageau, 2010). Among PcG genes, *Bmi1* plays a central role in the inheritance of the stemness of somatic stem cells, including hematopoietic stem cells (HSCs) and neural stem cells (Park et al., 2003; Iwama et al.,

2004; Molofsky et al., 2003), and its forced expression augments their self-renewal capability (Iwama et al., 2004). One of the major targets of *Bmi1* is the *Ink4a/Arf* tumor suppressor gene locus, and deletion of both *Ink4a* and *Arf* in *Bmi1*-deficient mice substantially restores the defective self-renewal capacity of HSCs (Oguro et al., 2006). PcG and trithorax-group proteins mark developmental regulator gene promoters with bivalent domains consisting of overlapping repressive and activating

© 2012 Oguro et al. This article is distributed under the terms of an Attribution-NonCommercial-Share Alike-No Mirror Sites license for the first six months after the publication date (see <http://www.rupress.org/terms>). After six months it is available under a Creative Commons License (Attribution-NonCommercial-Share Alike 3.0 Unported license, as described at <http://creativecommons.org/licenses/by-nc-sa/3.0/>).

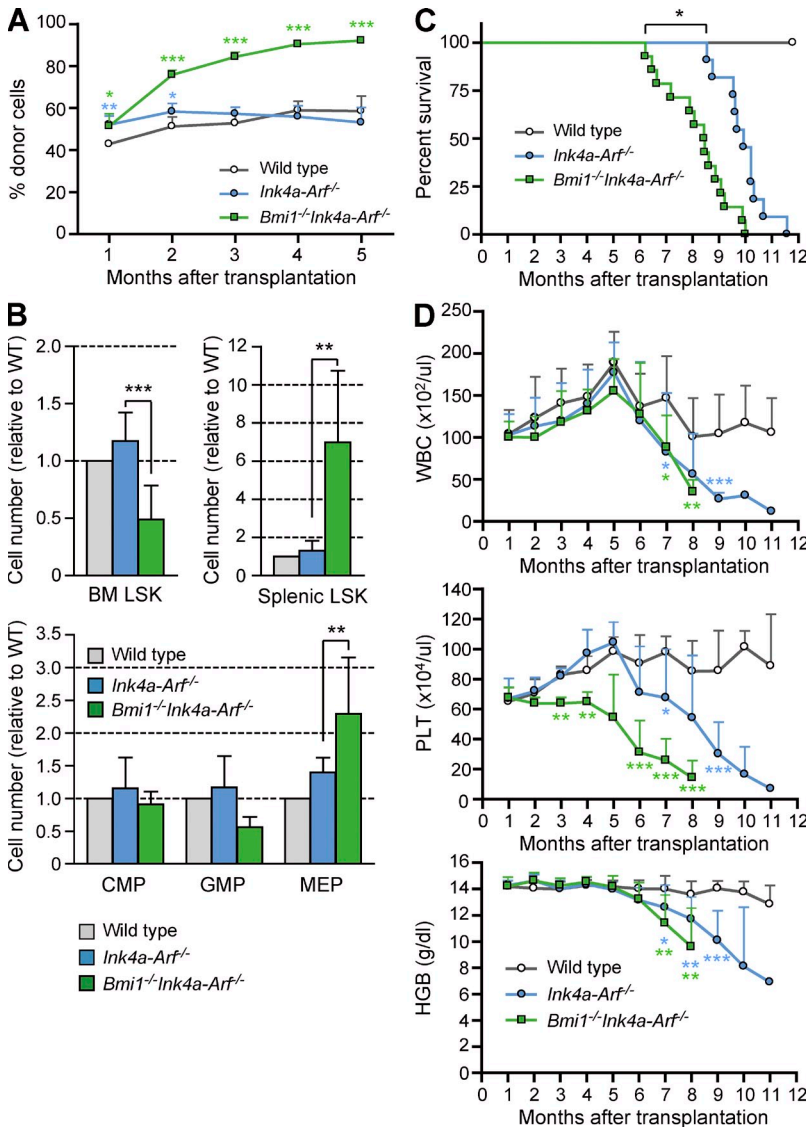
H. Oguro and J. Yuan contributed equally to this paper.

histone modifications to keep them poised for activation in embryonic stem cells (Pietersen and van Lohuizen, 2008; Konuma et al., 2010). Likewise, we found that *Bmi1* reinforces bivalent histone domains at key hematopoietic regulator gene promoters in multipotent hematopoietic stem and progenitor cells to maintain their multipotency (Oguro et al., 2010). Thus, *Bmi1* functions in the maintenance of both the self-renewal capacity and multipotency of HSCs.

Bmi1 has also been implicated in the maintenance of the proliferative capacity of leukemic stem cells (LSCs). Co-expression of *HoxA9* and *Meis1*, which can transform HSCs, induces leukemia from *Bmi1*-deficient fetal liver cells in primary recipient mice, but fails to sustain a leukemic state in the secondary recipients (Lessard and Sauvageau, 2003), suggesting that *Bmi1* regulates the self-renewal of both HSCs and LSCs. In addition, we have recently reported that *Bmi1* is essential for the faithful reprogramming of myeloid progenitors into LSCs, and that leukemic fusion genes require

PcG proteins acting in concert to establish LSC-specific transcriptional profiles that confer full leukemogenic activity on LSCs (Yuan et al., 2011). Notably, a gain-of-function mutation of the PRC2 gene, *EZH2*, has recently been identified in a subset of lymphoma (Morin et al., 2010), highlighting the oncogenic properties of PRC2 genes. In contrast, inactivating mutations of *EZH2* have also been identified in patients with myelodysplastic syndrome and myeloproliferative neoplasms (MPN), revealing that *EZH2* also has a tumor suppressor function (Ernst et al., 2010; Nikoloski et al., 2010).

In this study, we found that *Bmi1* antagonizes development of MPN in the absence of its major tumor-suppressive targets, *Ink4a* and *Arf*, and identified *Hmga2*, an oncogene, as one of the direct targets of *Bmi1* involved in the development of MPN. Our findings suggest that PcG genes fine-tune the hematopoietic homeostasis by balancing the transcription of oncogenic and tumor suppressive target genes.



RESULTS AND DISCUSSION

Loss of *Bmi1* augments repopulating capacity of BM cells in an *Ink4a/Arf*-null background

We previously reported that deletion of both *Ink4a* and *Arf* in *Bmi1*-deficient mice substantially restores the defective self-renewal capacity of HSCs (Oguro et al., 2006). In this study, we performed competitive repopulation assays using the same number of BM competitor cells as the test cells, and found that *Bmi1*^{-/-}*Ink4a-Arf*^{-/-} cells had higher repopulating activity in recipient mice than the wild-type and *Ink4a-Arf*^{-/-}

Figure 1. Loss of *Bmi1* augments the repopulating capacity of BM cells in the absence of *Ink4a/Arf*.

(A) To perform a competitive repopulating assay, 10⁶ pooled test BM cells from 4-wk-old mice (CD45.2⁺) of the indicated genotype were mixed with 10⁶ competitor BM cells (CD45.1⁺) and injected into lethally irradiated recipient mice (CD45.1⁺). The percent chimerism of donor cells in the recipient PB is presented as the mean ± SD (n = 5). *, P < 0.05; **, P < 0.01; ***, P < 0.001. (B) Relative numbers of donor-derived BM and splenic LSK cells, and BM CMPs, GMPs, and MEPs. Lethally irradiated wild-type recipient mice were infused with 2 × 10⁶ BM cells of the indicated genotype and analyzed at 4 mo after transplantation. Data were normalized relative to wild type and are shown as the mean ± SD (BM LSK cells, n = 12; splenic LSK cells, n = 6; CMPs, GMPs, and MEPs, n = 5; *, P < 0.05; **, P < 0.01; ***, P < 0.001). (C) Survival curve of the wild-type recipient mice repopulated by BM cells from indicated mutant mice. The data from four independent experiments were combined (wild type, n = 12; *Ink4a-Arf*^{-/-}, n = 11; *Bmi1*^{-/-}*Ink4a-Arf*^{-/-}, n = 14). The significance of the difference in survival curves was calculated by log-rank test. *, P = 0.0007. (D) PB analysis of white blood cells (WBC), platelets (PLT), and hemoglobin (HGB) of the wild-type recipient mice in C. Data are shown as the mean ± SD. *, P < 0.05; **, P < 0.01; ***, P < 0.001.

control BM cells (Fig. 1 A). To evaluate the repopulating capacity of *Bmi1*^{-/-}*Ink4a-Arf*^{-/-} BM cells precisely, we then transplanted wild-type, *Ink4a-Arf*^{-/-}, and *Bmi1*^{-/-}*Ink4a-Arf*^{-/-} BM cells into lethally irradiated mice without competitor cells. At 4 mo after transplantation, the recipients repopulated with *Bmi1*^{-/-}*Ink4a-Arf*^{-/-} donor cells had significantly fewer lineage marker-negative (Lineage⁻) Sca-1⁺c-Kit⁺ (LSK) cells in BM than did the control recipients as we reported previously (Oguro et al., 2010; Fig. 1 B). However, they had twofold more megakaryocyte/erythroid progenitors (MEPs) than the controls (Fig. 1 B) and showed extramedullary hematopoiesis as evident from a significant increase in the number of LSK HSCs/multipotent progenitors

(MPPs) in spleen (Fig. 1 B). All of the recipient mice repopulated with *Ink4a-Arf*^{-/-} BM cells eventually developed sarcomas or lymphomas and died by 11 mo after transplant, as reported with the *Ink4a-Arf*^{-/-} mice (Fig. 1 C; Serrano et al., 1996). Alternatively, the recipient mice repopulated with *Bmi1*^{-/-}*Ink4a-Arf*^{-/-} BM cells died much earlier than the *Ink4a-Arf*^{-/-} controls (Fig. 1 C) and displayed a more progressive thrombocytopenia (Fig. 1 D).

***Bmi1*-deficient hematopoietic cells induce lethal myelofibrosis**

The recipient mice repopulated by *Bmi1*^{-/-}*Ink4a-Arf*^{-/-} BM cells had marked hepatosplenomegaly (not depicted) and hypoplastic BM with severe fibrosis (Fig. 2, A and B) at their

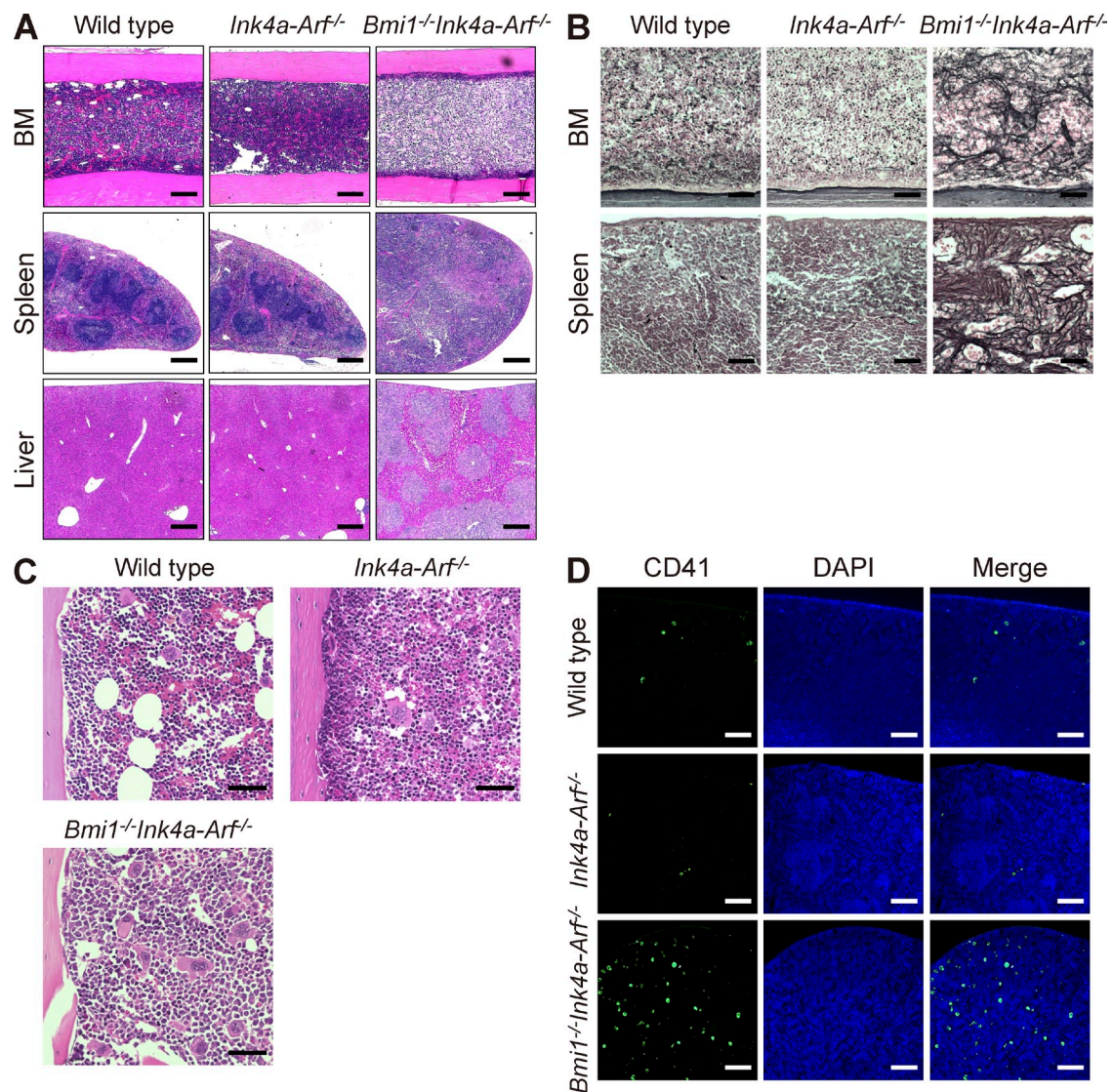


Figure 2. Enhanced megakaryocytopoiesis and massive myelofibrosis induced by *Bmi1*^{-/-}*Ink4a-Arf*^{-/-} hematopoietic cells. (A) Hematoxylin and eosin (H&E) staining of BM, spleen, and liver sections. BM, spleen, and liver of representative wild-type recipient mice repopulated by 2×10^6 BM cells of the indicated genotype were analyzed at 174 d after transplantation. Bars: 125 μm (BM); 500 μm (spleen and liver). (B) Silver staining of BM and spleen sections in A. Bars, 50 μm. (C) H&E staining of BM sections of representative recipient mice repopulated with the indicated mutant BM cells analyzed at 138 d after transplantation. Bars, 50 μm. (D) CD41 (green) and DAPI (blue) staining of spleen sections of representative recipient mice repopulated with indicated mutant BM cells analyzed at 138 d after transplantation. Bars, 125 μm.

terminal stage. The spleen structure was destroyed by extramedullary hematopoiesis accompanied by massive fibrosis (Fig. 2, A and B). Extramedullary hematopoiesis was also evident in the liver (Fig. 2 A). All these features resemble those of human primary myelofibrosis (PMF). Notably, the recipient mice infused with *Bmi1*^{-/-}*Ink4a-Arf*^{-/-} BM cells along with competitor cells in Fig. 1 A also developed lethal myelofibrosis in a similar fashion (not depicted).

PMF is the rarest and most severe chronic MPN (Tefferi et al., 2007; Levine and Gilliland, 2008). Abnormal megakaryocytosis in the BM has been proposed as the main causative factor for myelofibrosis. Deregulated stem cell signaling, resulting in part from mutated JAK2 and MPL, likely cause abnormal megakaryocytosis. Myelofibrosis is thought to be the consequence of an excessive release/leakage of growth factors within the BM by cells from pathological hematopoietic clones, especially by necrotic megakaryocytes. TGF- β 1 is speculated to be one of the major causative growth factors that activate mesenchymal cells (Martyr  et al, 1994). Although abnormal megakaryocytosis was obscure in BM and spleen because of severe fibrosis at the terminal stage of the disease, the mice at earlier time points after transplantation had marked megakaryocytosis in both BM and spleen (Fig. 2, C and D). These findings clearly implicate pathological megakaryocytosis in the development of lethal myelofibrosis, and indicate that lethal myelofibrosis induced by *Bmi1*^{-/-}*Ink4a-Arf*^{-/-} hematopoietic cells follows the natural course of human PMF.

Derepression of *Hmga2* in *Bmi1*-deficient hematopoietic stem/progenitor cells

To identify the genes responsible for PMF-like disease in the absence of *Bmi1*, we compared gene expression profiles of LSK HSCs/MPPs and common myeloid progenitors (CMPs). In total, 245 and 286 genes were derepressed by more than twofold, specifically in *Bmi1*^{-/-}*Ink4a-Arf*^{-/-} LSKs and CMPs, respectively (Fig. 3 A). We then compared the list of derepressed genes with a list of PMF-associated genes identified by gene expression profiling of CD34⁺ cells in human PMF patients (Guglielmelli et al., 2007). *Hmga2* appeared to be commonly up-regulated in *Bmi1*^{-/-}*Ink4a-Arf*^{-/-} CMPs and PMF CD34⁺ cells. *HMGGA2* was found to be one of eight genes that can distinguish PMF CD34⁺ cells from normal CD34⁺ cells, and abnormal expression of *HMGGA2* was associated with the presence of *JAK2*^{V617F} (Guglielmelli et al., 2007). Moreover, overexpression of *HMGGA2* was reported in 12 of 12 patients with myelofibrosis with myeloid metaplasia, among which two patients had a chromosomal translocation involving the *HMGGA2* gene at 12q (Andrieux et al., 2004). We therefore focused on *Hmga2*. *Hmga2* expression was up-regulated by 1.6- and 13.4-fold in *Bmi1*^{-/-}*Ink4a-Arf*^{-/-} LSKs and CMPs, respectively, in our microarray analysis (Fig. 3 A). We then quantified the *Hmga2* expression in each progenitor fraction by quantitative RT-PCR. Because the BM environment of *Bmi1*^{-/-} and *Bmi1*^{-/-}*Ink4a-Arf*^{-/-} mice is defective in supporting HSCs (Oguro et al., 2006), we purified progenitors from wild-type recipient BM reconstituted

with wild-type, *Ink4a-Arf*^{-/-}, or *Bmi1*^{-/-}*Ink4a-Arf*^{-/-} BM cells to exclude any environmental effects. *Hmga2* expression was predominantly found in CMPs in wild-type mice, but in the absence of *Bmi1*, it was derepressed in Flt3⁻LSK HSCs/MPPs (2.4-fold compared with *Ink4a-Arf*^{-/-} cells) and markedly increased in myeloid-committed progenitors (CMPs, 14.1-fold; granulocyte/macrophage progenitors [GMPs], 268-fold; MEPs, 11.5-fold), but was barely affected in Flt3⁺LSK lymphoid-primed MPPs (LMPPs, 0.9-fold) or common lymphoid progenitors (CLPs, 0.74-fold; Fig. 3 B). To confirm that this derepression is in fact mediated by loss of *Bmi1*, we performed RT-PCR analysis on Lineage⁻c-Kit⁺ *Bmi1*^{-/-} progenitors and found that *Hmga2*, as well as the canonical targets *Ink4a* and *Arf*, are derepressed in a *Bmi1*-deficient setting (Fig. 3 C). These results suggest that *Bmi1* functions in the silencing of *Hmga2* in cell types ranging from HSCs to myeloid progenitors.

Direct repression of *Hmga2* transcription by *Bmi1*

The high-mobility group A (HMGA) nonhistone chromatin proteins alter chromatin structure, and thereby regulate transcription. HMGA proteins have been implicated in both benign and malignant tumors through mechanisms that result in HMGA overexpression. Chromosomal rearrangements involving the region 12q13-15, in which the *HMGGA2* gene is located, are one of the major mechanisms causing deregulation of the *HMGGA2* gene, giving rise to a truncated transcript lacking the C-terminal tail and/or 3'-UTR. Expression of *HMGGA2* is negatively regulated by the let-7 family of microRNAs, which bind to the 3'-UTR of *HMGGA2* and restrict its expression. Thus, chromosomal rearrangements within the *HMGGA2* locus cause overexpression of a full-length or truncated HMGA2 with a preserved DNA-binding capacity (Fusco and Fedele, 2007; Young and Narita, 2007).

To examine whether *Bmi1* directly represses transcription of *Hmga2*, we next characterized the *Hmga2* promoter by conducting chromatin immunoprecipitation (ChIP) assays. To obtain enough cells, we used BM Lineage⁻c-Kit⁺ progenitors depleted of cells committed to the lymphoid, myeloid, and erythroid lineages. Binding of *Bmi1* to the *Hmga2* promoter was detected, but not to the promoter of the control gene, β -actin (Fig. 3 D), which was marked with H3K4me3, an active histone mark (not depicted). PRC1 catalyzes the monoubiquitination of histone H2A (H2Aub1) at lysine 119. The *Hmga2* promoter was marked with H2Aub1 in wild-type BM Lineage⁻c-Kit⁺ progenitors (Fig. 3 D). The levels of *Bmi1* binding and H2Aub were significantly reduced in *Bmi1*^{-/-}*Ink4a-Arf*^{-/-} Lineage⁻ progenitors compared with the levels in wild-type cells (Fig. 3 E). These results indicate that *Bmi1* directly represses the expression of *Hmga2* by marking its promoter with a repressive histone mark.

Hmga2 promotes expansion of progenitor cells and enhances megakaryocytopoiesis in vitro

The specific up-regulation of *HMGGA2* expression in PMF, but not in other chronic MPNs, such as polycythemia vera

and essential thrombocythemia, suggested a contribution of *HMGA2* to the development and/or progression of PMF (Guglielmelli et al., 2007). To address this, we evaluated the proliferative and differentiation capacity of *Hmga2*-overexpressing CD34⁺LSK HSCs. In all experiments, transduction efficiency was ~90% as determined by flow cytometry

using GFP as a marker (unpublished data). In liquid cultures supplemented with SCF, TPO, IL-3, IL-6/IL-6 receptor fusion protein (FP6), and EPO, *Hmga2*-overexpressing HSCs showed a growth advantage compared with the control (Fig. 4 A), and the *Hmga2* culture contained significantly more LSK cells than the control at day 10 of culture

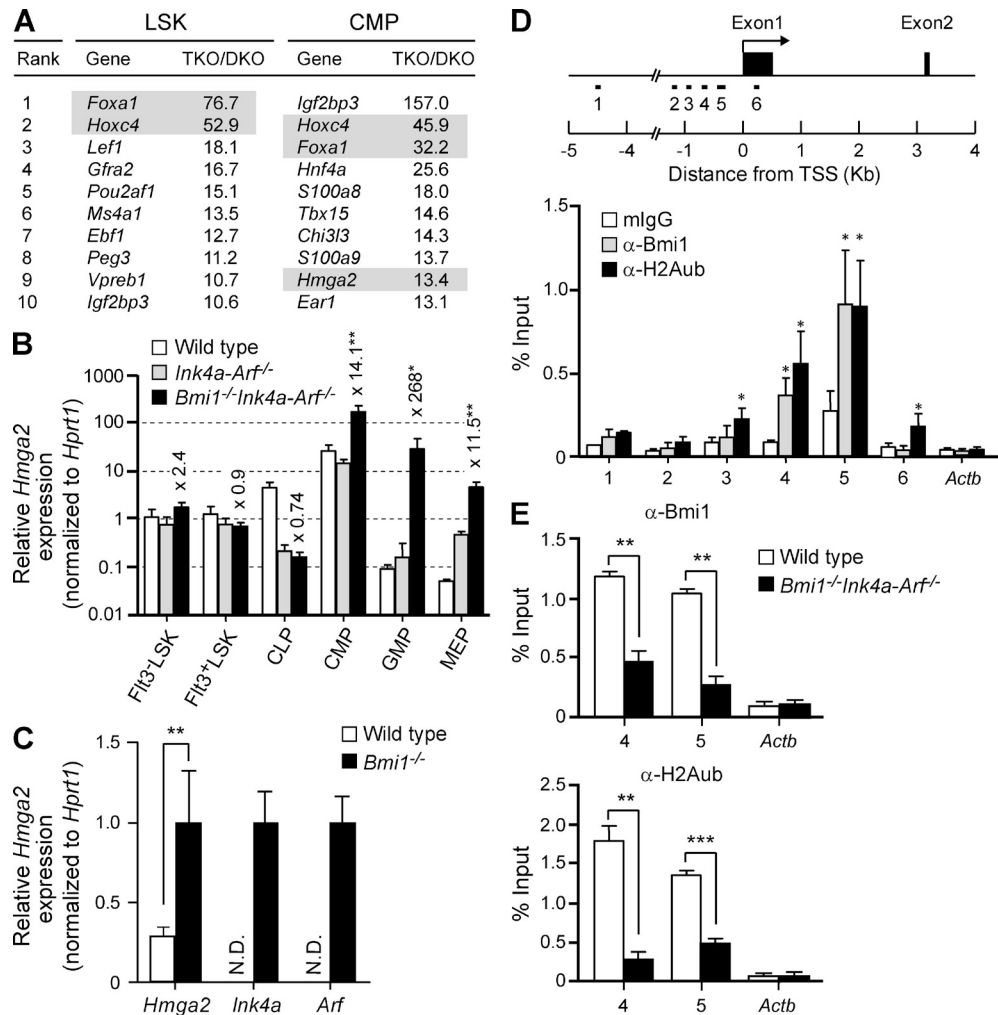


Figure 3. Derepression of *Hmga2* in *Bmi1*^{-/-}*Ink4a-Arf*^{-/-} hematopoietic cells. (A) List of top 10 genes up-regulated in LSK cells and CMPs in the absence of Bmi1. IL-7R α LSK cells purified from BM of 4-wk-old *Ink4a-Arf*^{-/-} (DKO) and *Bmi1*^{-/-}*Ink4a-Arf*^{-/-} (TKO) mice and CMPs from recipients' BM at 4 mo after infusion of DKO and TKO BM cells were subjected to microarray analyses and their profiles were compared. Highlighted genes were further characterized in this study. (B) Quantitative RT-PCR analysis of *Hmga2* expression. mRNA levels in each progenitor fraction from the recipients' BM repopulated by BM cells of the indicated genotype at 4 mo after transplantation were normalized to *Hprt1* expression. Expression levels relative to those in the wild-type Flt3⁺ LSK cells are shown as the mean \pm SD for triplicate analyses. The fold change in expression levels between *Bmi1*^{-/-}*Ink4a-Arf*^{-/-} cells and *Ink4a-Arf*^{-/-} cells is also indicated. *, $P < 0.05$; **, $P < 0.01$. (C) Derepression of *Hmga2* in *Bmi1*-deficient hematopoietic cells. Lineage⁻c-Kit⁺ cells were purified from BM of 4-wk-old wild-type and *Bmi1*^{-/-} mice. mRNA levels of *Hmga2*, *Ink4a*, and *Arf* were normalized to *Hprt1* expression. Expression levels relative to those in the *Bmi1*^{-/-} cells are shown as the mean \pm SD for triplicate analyses. N.D. indicates not detected. **, $P < 0.01$. (D) ChIP analysis at the *Hmga2* promoter in wild-type Lineage⁻c-Kit⁺ cells. The *Hmga2* locus indicating its genomic structure (based on the Ensemble data, transcript ID ENSMUST00000072777) is depicted in the top panel. Exons are demarcated by black boxes. The regions 1–6 amplified from the precipitated DNA by site-specific quantitative PCR are indicated. The binding of Bmi1 and the levels of H2Aub were determined by ChIP using control mouse IgG (mlgG), anti-Bmi1, and anti-H2Aub antibodies and site-specific real-time PCR. The relative amount of immunoprecipitated DNA is presented as a percentage of input DNA (bottom). The data are shown as the mean \pm SD for four independent experiments. The β -actin promoter (*Actb*) served as a negative control. *, $P < 0.05$. (E) ChIP analysis at the *Hmga2* promoter in wild-type or *Bmi1*^{-/-}*Ink4a-Arf*^{-/-} Lineage⁻ cells. The binding of Bmi1 and the levels of H2Aub were determined by ChIP using anti-Bmi1 or anti-H2Aub antibodies and site-specific real-time PCR as in D. The data are shown as the mean \pm SD for triplicate PCRs from two independent experiments. *, $P < 0.05$; **, $P < 0.01$; ***, $P < 0.001$.

(Fig. 4 B). Morphological analysis unveiled a drastic enhancement in production of megakaryocytes upon the overexpression of *Hmga2*. The *Hmga2* culture contained significantly more multinucleated megakaryocytes and mononuclear micromegakaryocytes (Fig. 4, C and D).

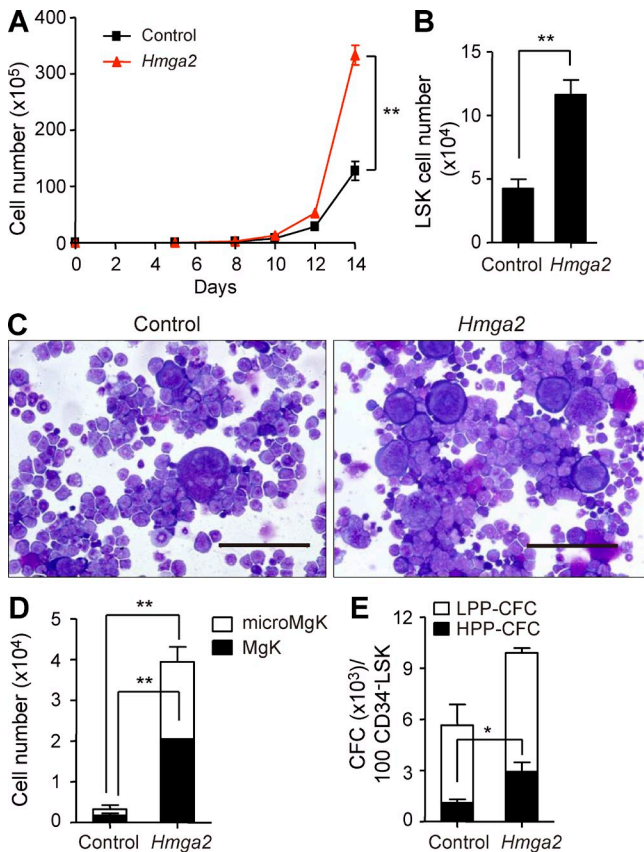


Figure 4. *Hmga2* promotes expansion of progenitor cells and enhances megakaryocytopoiesis in vitro. (A) Growth of CD34⁺-LSK HSCs transduced with the *Hmga2* retrovirus. 100 CD34⁺-LSK HSCs were transduced with either the empty vector or *Hmga2* retrovirus and cultured in the presence of SCF, TPO, IL-3, FP6, and EPO for 14 d. Numbers of cells are shown as the mean \pm SD for triplicate cultures. **, $P < 0.01$. (B) Number of LSK cells in culture. Flow cytometric analysis of the culture in A was performed at day 10 of culture. Absolute numbers of LSK cells are indicated as the mean \pm SD ($n = 3$). **, $P < 0.01$. (C) Morphology of CD34⁺-LSK HSCs at day 12 of culture. CD34⁺-LSK HSCs transduced with the indicated retroviruses in A were recovered, cytospun onto slide glasses, and subjected to May-Grünwald Giemsa staining. The morphology of the cells was observed under a light microscope. Bars, 100 μ m. (D) The frequency of multinucleated megakaryocytes (MgK) and mononuclear micromegakaryocytes (microMgK) in culture. The cytospun cells on slide glasses in C were examined under a light microscope and absolute numbers in culture are indicated as the mean \pm SD. Counts of 500 cells were independently performed three times. **, $P < 0.01$. (E) Effect of *Hmga2* on CFC numbers in culture. 100 CD34⁺-LSK HSCs were transduced with the indicated retrovirus and cultured in the presence of SCF and TPO. At day 10 of culture, colony assays were performed to evaluate the number of CFCs in culture. Absolute numbers of low proliferative potential (LPP; diameter < 1 mm) and HPP (diameter ≥ 1 mm) CFCs are shown as the mean \pm SD for triplicate cultures. *, $P < 0.05$; **, $P < 0.01$.

We then cultured transduced HSCs for 9 d (10 d of culture in total) in the presence of SCF and TPO, which supports the proliferation of HSCs and progenitors rather than their differentiation (Ema et al., 2000). The total number of colony-forming cells (CFCs) was significantly increased in the *Hmga2* culture (Fig. 4 E). Among CFCs, the number of high proliferative potential (HPP)-CFCs, which generate a colony with a diameter > 1 mm, was increased with *Hmga2* compared with the control. These results indicate that overexpression of *Hmga2* promotes expansion of progenitor cells and also facilitates the proliferation and differentiation of megakaryocytic cells in vitro.

Forced expression of *Hmga2* promotes megakaryocytopoiesis and induces myeloproliferative hematopoiesis in vivo

We next examined the effect of *Hmga2* overexpression on hematopoiesis in vivo. We performed competitive repopulation assays using 30 CD34⁺-LSK HSCs transduced with *Hmga2* (CD45.2) at day 3.5 of culture along with 2×10^5 fresh unfractionated BM cells (CD45.1) for radioprotection. *Hmga2*-overexpressing cells showed a greater, albeit not statistically significant, contribution to the myeloid lineage in peripheral blood (PB) compared with the control (Fig. 5 A). Recipients repopulated with *Hmga2*-overexpressing cells had significantly more LSK cells and myeloid progenitors in BM compared with the control (Fig. 5 C). Furthermore, they also had mild splenomegaly with extramedullary hematopoiesis as evident from a marginal increase in LSK HSCs/MPPs in the spleen and a significant increase in the PB (Fig. 5 B and C). The recipients repopulated with *Hmga2*-overexpressing cells appeared to have more megakaryocytes in the BM (not depicted) and platelets in the PB (Fig. 5 D). These findings indicate that derepression of *Hmga2* could induce an MPN-like state with enhanced megakaryocytopoiesis and correspond well with findings recently obtained with transgenic mice carrying a 3'-UTR-truncated *Hmga2* cDNA ($\Delta Hmga2$ mice; Ikeda et al., 2011). $\Delta Hmga2$ mice developed MPN-like hematopoiesis with an increased number of megakaryocytes in the BM, although the number of platelets in the PB was not described. Together, these findings implicate *Hmga2* in the PMF-like pathological hematopoiesis induced by *Bmi1*^{-/-} *Ink4a-Arf*^{-/-} BM cells.

Given that *HMGA2* is highly derepressed in CD34⁺ stem and progenitor cells in PMF patients, PcG function could be compromised in PMF patients, partly by loss-of-function mutations of *EZH2*. Indeed, we confirmed that *Ezh2* also regulates *Hmga2* as *Bmi1* does. *Hmga2* was highly derepressed in *Ezh2*-deficient progenitor cells (unpublished data). ChIP assays demonstrated that the *Hmga2* promoter is bound by *Ezh2* and marked with H3K27me3 in wild-type BM Lineage⁻ *c-Kit*⁺ progenitors (unpublished data). Interestingly, recipient mice repopulated with *Ezh2*-deficient BM cells showed an increase in the platelet count in PB similar to recipients repopulated with HSCs overexpressing *Hmga2* (Mochizuki-Kashio et al., 2011). These data indicate that both *Bmi1* and *Ezh2* transcriptionally repress *Hmga2*. However, the

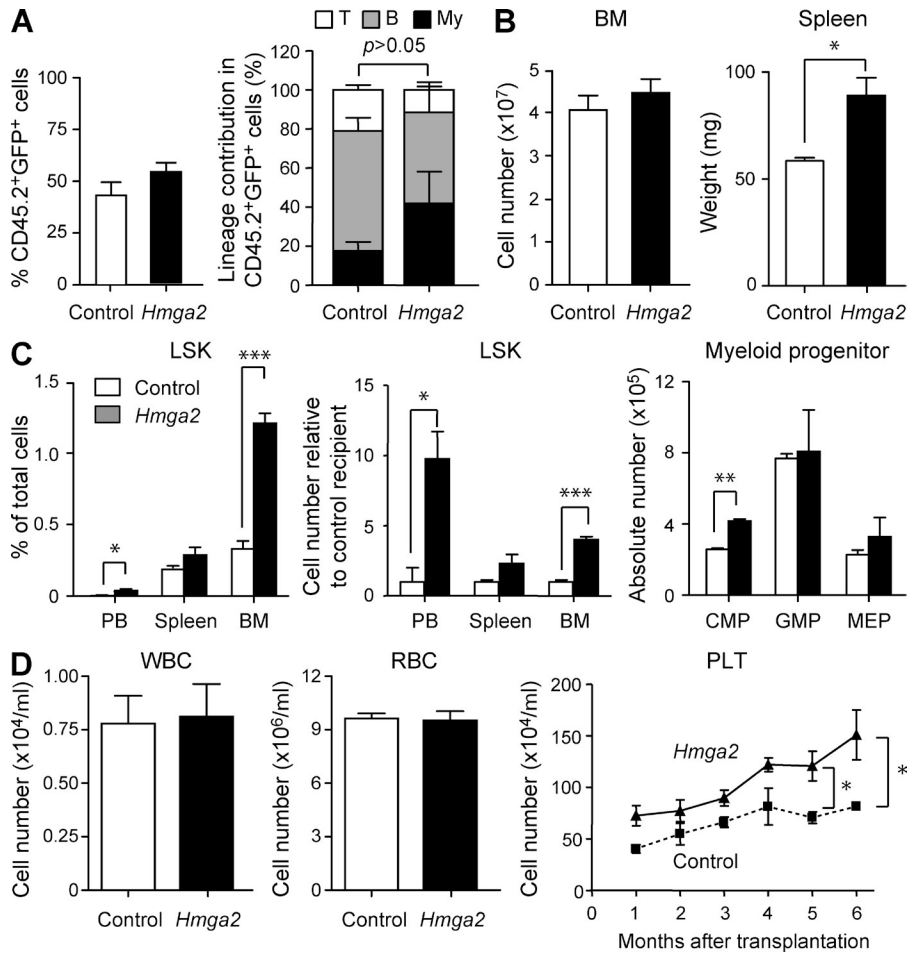


Figure 5. Forced expression of *Hmga2* causes myeloproliferative hematopoiesis with enhanced megakaryocytopoiesis.

(A) Donor chimerism and lineage contribution in PB ($n = 5$). CD34⁻LSK HSCs (CD45.2) transduced with either control or *Hmga2* retrovirus were transplanted into lethally irradiated CD45.1 mice together with 2×10^5 BM competitor cells from 8-wk-old CD45.1 mice. The chimerism of CD45.2⁺GFP⁺-transduced cells in PB of recipient mice was examined at 6 mo after transplantation (left). Lineage contribution of CD45.2⁺GFP⁺ donor cells to myeloid (Gr-1⁺ and/or Mac-1⁺), B (B220⁺), or T (CD4⁺ or CD8⁺) cells (right). Data are presented as the mean \pm SD ($n = 6$). (B) Absolute numbers of BM mononuclear cells (from bilateral femurs and tibiae) and spleen weights at 6 mo after transplantation. Data are presented as the mean \pm SD ($n = 6$). *, $P < 0.05$. (C) Frequency of LSK cells and absolute numbers of myeloid progenitor cells in BM. The frequency of LSK cells in PB, BM, and spleen (left) and absolute numbers of myeloid progenitor cells in BM (right) of recipient mice examined 6 mo after transplantation. The relative number of LSK cells is presented in the middle panel. Data are presented as the mean \pm SD ($n = 6$). *, $P < 0.05$; **, $P < 0.01$; ***, $P < 0.001$. (D) PB cell counts of recipients repopulated with CD34⁻LSK HSCs transduced with the indicated retrovirus. Cell counts at 6 mo after transplantation are presented for white blood cells (WBC) and red blood cells (RBC). The time course of the increase in platelet (PLT) counts is also depicted. Data are presented as the mean \pm SD ($n = 6$). *, $P < 0.05$.

frequency of *EZH2* mutations in PMF has been reported to be only 13% (Nikoloski et al., 2010). Thus, it would be intriguing to examine other mechanisms that compromise PcG function in PMF patients without *EZH2* mutations.

Nevertheless, it should be noted that *Hmga2* is not the only oncogenic target of *Bmi1* responsible for the establishment of PMF-like disease, as fibrosis was not seen in recipient BM that was repopulated with *Hmga2*-overexpressing cells at 6 mo after transplantation (unpublished data). As evident from the significant increase in platelet counts, overexpression of *Hmga2* does not compromise the terminal differentiation of megakaryocytes. It has been proposed that necrotic megakaryocytes in BM are the main causative factor for myelofibrosis. Although derepression of *Hmga2* induces an MPN-like state with enhanced megakaryocytopoiesis, it may require the derepression of other *Bmi1* targets to eventually induce a fibrotic state after a preceding MPN-like state. Our microarray analysis also identified *Hoxc4* and *Foxa1* as being derepressed in *Bmi1*^{-/-}*Ink4a*-*Arf*^{-/-} cells (Fig. 3 A). We confirmed this derepression by RT-PCR (unpublished data), and *Hoxc4* and *Foxa1* also appeared to be direct targets of *Bmi1* by ChIP assays (unpublished data). We tested the effects of forced expression of these genes in HSCs, but failed to induce an MPN-like disease in recipient mice (unpublished data).

Collectively, our findings indicate that *Bmi1* antagonizes the development of MPN in the absence of its major tumor-suppressive targets, *Ink4a* and *Arf*, and we showed the tumor suppressive function of *Bmi1* through epigenetic silencing of oncogenes. Although *Bmi1*-deficiency is self-limiting unless *Ink4a* and *Arf* are deleted first, *INK4A* and *ARF* are frequently inactivated by deletions or mutations, or transcriptionally repressed by DNA methylation at their promoters in human cancers. Therefore, the situations like the *Ink4a*/*Arf*-null background that we used in this study also happen in the initiation and progression of human cancers. Our findings suggest that in such situations, the tumor cells with impaired BMI1 function could outcompete cells with normal BMI1 function because the effects of derepressed oncogenes, such as *HMGA2*, appear to supersede the effects of derepressed tumor suppressor genes. Corresponding to our findings, PRC1 has been reported to exert tumor suppressor activity through epigenetic silencing of Notch and JAK-STAT signaling in *Drosophila melanogaster* eyes (Martinez et al., 2009; Classen et al., 2009). Furthermore, mice with hypomorphic mutations of *Eed* and *Suz12* show enhanced hematopoiesis (Lessard et al., 1999; Majewski et al., 2008). All of these findings support the

tumor suppressor function of EZH2 observed in human myelodysplastic syndrome and MPN, and are suggestive of a broad range of target genes of the PcG proteins, including both oncogenes and tumor suppressor genes. Although tumor suppressor genes have been stressed as PcG targets, our findings shed light on the role of PcG proteins in the gene silencing of oncogenes. Thus, the PcG proteins fine-tune the growth of hematopoietic cells in both a positive and a negative manner to maintain hematopoietic homeostasis.

MATERIALS AND METHODS

Mice. *Bmi1*^{+/-} mice (van der Lugt et al., 1994) and *Ink4a-Arf*^{-/-} mice (Serrano et al., 1996) that had been backcrossed at least eight times onto a C57BL/6 (CD45.2) background were used. C57BL/6 (CD45.2) mice and C57BL/6 mice congenic for the Ly5 locus (CD45.1) were purchased from Japan SLC and Sankyo Laboratory Service, respectively. Littermates were used as controls in all experiments. All mice were bred and maintained in the Animal Research Facility of the Graduate School of Medicine, Chiba University in accordance with institutional guidelines. All experiments using mice received approval from the Chiba University Administrative Panel for Animal Care.

Competitive repopulation assay. BM cells (10⁶) from 4-wk-old CD45.2 mice were mixed with the same number of unfractionated BM competitor cells (CD45.1) and transplanted into CD45.1 mice irradiated at a dose of 9.5 Gy. PB cells of the recipient mice were analyzed with a mixture of antibodies that included PE-Cy7-conjugated anti-CD45.1, Pacific blue-conjugated anti-CD45.2, PE-conjugated anti-Mac-1 and anti-Gr-1, APC-conjugated anti-B220, and APC-Cy7-conjugated anti-CD4 and anti-CD8 α antibodies. Cells were analyzed on a FACSCanto II (BD). Donor cell chimerism in the recipient PB cells was evaluated as percent donor chimerism calculated as (percent donor cells) \times 100/(percent donor cells + percent recipient cells). PB cell counts were made using an automated cell counter (Celltec α ; Nihon Kohden).

Purification of mouse HSCs and progenitors. Mouse HSCs (CD34⁻LSK cells) were purified from BM of 8-wk-old mice. Mononuclear cells were isolated on Ficol-Paque PLUS (GE Healthcare). The cells were stained with an antibody cocktail consisting of biotinylated anti-Gr-1, Mac-1, IL-7R α , B220, CD4, CD8 α , and Ter119 monoclonal antibodies. Lineage⁺ cells were depleted with goat anti-rat IgG microbeads (Miltenyi Biotec) through an LD column (Miltenyi Biotec). The cells were further stained with FITC-conjugated anti-CD34, PE-conjugated anti-Sca-1, and APC-conjugated anti-c-Kit antibodies. Biotinylated antibodies were detected with APC-Cy7-conjugated streptavidin. Analysis and sorting were performed on a FACS Aria II (BD). CMPs, GMPs, MEPs, and CLPs were analyzed as CD34⁺Fc γ R^{low}c-Kit⁺Sca-1⁻Lineage⁻IL-7R α ⁻ cells, CD34⁺Fc γ R^{hi}c-Kit⁺Sca-1⁻Lineage⁻IL-7R α ⁻ cells, CD34⁻Fc γ R^{low}c-Kit⁺Sca-1⁻Lineage⁻IL-7R α ⁻ cells, and IL-7R α ⁺c-Kit^{low}Sca-1^{low}Lineage⁻ cells, respectively.

Retroviral vectors expressing *Hmga2* and virus production. Full-length mouse *Hmga2* cDNA in the pMY-ires-EGFP retroviral expression vector was kindly provided by K. Nakashima (Nara Institute of Science and Technology, Ikoma, Nara, Japan). A recombinant vesicular stomatitis virus glycoprotein (VSV-G)-pseudotyped high-titer retrovirus was generated by a 293gpg packaging cell line that had been engineered to express the VSV-G protein under the control of a tetracycline-inducible system. The virus in supernatants of 293gpg cells was concentrated by centrifugation at 6,000 g for 16 h. Viral titers were determined by infecting Jurkat cells (a human T cell line).

Transduction of CD34⁻LSK HSCs. CD34⁻LSK HSCs were transduced with the indicated retrovirus, as previously described, with minor modifications (Iwama et al., 2004). CD34⁻LSK HSCs were sorted into 96-well microtiter

plates coated with the recombinant human fibronectin fragment CH-296 (RetroNectin; Takara Shuzo) at 100 cells per well, and then incubated in α -MEM supplemented with 1% FBS, 1% L-glutamine, penicillin, streptomycin solution (GPS; Sigma-Aldrich), 50 μ M 2-mercaptoethanol (2-ME), 100 ng/ml mouse stem cell factor (SCF; PeproTech), and 100 ng/ml human thrombopoietin (TPO; PeproTech) for 24 h. Next, cells were transduced with the indicated retrovirus at a multiplicity of infection (MOI) of 1,500 in the presence of 1 μ g/ml RetroNectin and 10 μ g/ml protamine sulfate (Sigma-Aldrich) for 24 h. After transduction, cells were further incubated in the same medium for 9 d, subjected to in vitro colony assays or in S-Clone SF-O3 (Sanko Junyaku) supplemented with 0.2% BSA, 50 μ M 2-ME, 1% GPS, 50 ng/ml SCF, and 50 ng/ml TPO for 2.5 d, and then subjected to competitive repopulation assays. The transduction efficiency was nearly 90%, as judged from GFP expression. Colony assays were performed using a methylcellulose medium (M3234; STEMCELL Technologies) supplemented with 20 ng/ml mouse SCF, 20 ng/ml mouse IL-3 (PeproTech), 50 ng/ml human TPO, and 3 U/ml human EPO (provided by Kyowa Hakko Kirin). Colony numbers were counted on day 10. CD34⁻LSK HSCs (CD45.2) transduced with the indicated retrovirus were also transplanted intravenously into 8-wk-old CD45.1 mice irradiated at a dose of 9.5 Gy, together with 2 \times 10⁵ BM competitor cells from 8-wk-old CD45.1 mice.

Microarray analysis. IL-7R α ⁻LSK cells were purified from BM of 4-wk-old *Ink4a-Arf*^{-/-} and *Bmi1*^{-/-}*Ink4a-Arf*^{-/-} mice and CMPs from recipients' BM at 4 mo after infusion of *Ink4a-Arf*^{-/-} or *Bmi1*^{-/-}*Ink4a-Arf*^{-/-} BM cells. Total RNA was isolated using TRIZOL LS Reagent (Invitrogen), and its integrity was confirmed using LabChip RNA 6000 Nano chips and a 2100 Bioanalyzer (Agilent Technologies). Target cRNA was prepared from the total RNA equivalent to 10,000 cells (IL-7R α LSK) or 8,000 cells (CMPs) with a two-cycle cDNA synthesis kit and 3'-amplification reagents for IVT labeling (Affymetrix), and then hybridized to a GeneChip Mouse Genome 430 2.0 oligonucleotide microarray (Affymetrix) according to the manufacturer's instructions. The expression value of each gene was calculated and normalized using GeneChip Operating Software version 1.4 (Affymetrix). All data are MIAME compliant, and the raw data were deposited in Gene Expression Omnibus (accession no. GSE19796 and GSE31086).

Quantitative reverse transcription (RT) PCR analysis. Total RNA was isolated using TRIZOL LS solution (Invitrogen) and reverse transcribed by the ThermoScript RT-PCR system (Invitrogen) with an oligo dT primer. Real-time quantitative PCR was performed with an ABI prism 7300 Thermal Cycler (Applied Biosystems) using FastStart Universal Probe Master (Roche). *Hypoxanthine-guanosine phosphoribosyl transferase 1 (Hprt1)* expression was used to calculate relative expression levels. The combination of primer sequences and probe numbers are as follows: *Hmga2*, probe #26, 5'-AAG-GCAGCAAAAACAAGAGC-3' and 5'-CCGTTTTTCTCCAATGG-TCT-3'; *Hprt1*, probe #95, 5'-TCCTCCTCAGACCGCTTTT-3' and 5'-CCTGGTTCATCATCGCTAATC-3'.

ChIP assay. Lineage⁻ or Lineage⁻c-Kit⁺ BM cells (2 \times 10⁵ cells/antibody) isolated by flow cytometry were cross-linked with 1% formaldehyde for 15 min at room temperature, and incubated for 5 min at 4°C after the addition of 0.125 M glycine. Cells were washed with PBS, lysed with cell lysis buffer (50 mM Tris-HCl, pH 8.0, 10 mM EDTA, 150 mM NaCl, 0.5% SDS, and protease inhibitor cocktail [PIC; Roche]) on ice, and sonicated until the DNA fragments were 200–500 bp in mean size as measured by Bioruptor (Cosmo Bio). After centrifugation at 15,000 rpm for 10 min, sheared chromatin was diluted 10-fold in dilution buffer (50 mM Tris-HCl, pH 8.0, 150 mM NaCl, 1.1% Triton X-100, 0.11% sodium deoxycholate, and PIC), and precleared by addition of Dynabeads Protein G (Invitrogen) for 1 h at 4°C. For anti-Bmi1 (clone 8A9; provided by N. Nozaki, MAB Institute, Yokosuka, Kanagawa, Japan), precleared chromatin was immunoprecipitated overnight at 4°C with antibody/Dynabeads Protein G mix. For anti-ubiquityl-Histone H2A (H2Aub; clone E6C5, 05–678; Millipore), precleared chromatin was immunoprecipitated overnight at 4°C with anti-H2Aub, followed by the

addition of anti-mouse IgM μ (12-488; Millipore)/Dynabeads Protein G mix and incubation for 2 h at 4°C. Beads were then sequentially washed with the following combination of wash buffers; twice each with low-salt wash buffer (50 mM Tris-HCl, pH 8.0, 150 mM NaCl, 1 mM EDTA, 1% Triton X-100, 0.1% SDS, and 0.1% sodium deoxycholate), high-salt wash buffer (50 mM Tris-HCl, pH 8.0, 500 mM NaCl, 1 mM EDTA, 1% Triton X-100, 0.1% SDS, and 0.1% sodium deoxycholate), and LiCl wash buffer (10 mM Tris-HCl, pH 8.0, 250 mM LiCl, 1 mM EDTA, 0.5% NP-40, and 0.5% sodium deoxycholate). Bound chromatin was eluted and, together with input DNA, cross-linking was reversed in elution buffer (50 mM Tris-HCl, pH 8.0, 10 mM EDTA, and 1% SDS) by overnight incubation at 65°C. Immunoprecipitated DNA and input DNA were treated with RNaseA (Sigma-Aldrich) and proteinase K (Roche), and extracted with phenol:chloroform. Quantitative PCR analysis was performed using SYBR Premix Ex Taq II (Takara Bio), and the 7500/7500 Fast Real-Time PCR system (Applied Biosystems). Primer sequences are as follows: *Hmga2*, region 1, 5'-GGGA-AGCCAGCAGAGGTAAGCC-3' and 5'-CGAGCGCATTTCGACG-GCTC-3'; region 2, 5'-CTGGCACCATCGTGTGTCTGG-3' and 5'-TGCGCGCACACACTTCACT-3'; region 3, 5'-GGTCGCTCT-TTCCCGGGGC-3' and 5'-TCCACCGAGGGTTGCCCG-3'; region 4, 5'-GCCCGCTTCGAGGCAGTTGT-3' and 5'-CAAGAGGAGGG-GGCAGCCCA-3'; region 5, 5'-AAAACCTGGGCTCCGGGTGC-AGA-3' and 5'-GGCGGCCAGCTCAGCTCTAG-3'; region 6, 5'-CG-CTGGACGTCCGGTGTGAT-3' and 5'-AAGAGCGGCGAGAGCAG-GCG-3'; *Actb*, 5'-CCCAACACACTAGCAAATTAGAACCAC-3' and 5'-CCTGGATTGAATGGACAGAGACTCACT-3'.

Immunofluorescence staining of spleen. Frozen spleen sections were prepared and immunostained according to the method described by Kawamoto (2003). After fixation with 100% ethanol-dry ice and blocking in MAXblock medium (Active Motif) for 1 h at room temperature, spleen sections were incubated with a FITC-conjugated anti-CD41 antibody (BD) for 12 h at 4°C. Spleen sections were then washed and incubated with the DNA marker DAPI for 5 min at room temperature.

We thank M. van Lohuizen and R.A. DePinho for providing *Bmi1*^{-/-} mice and *Ink4a-Arf*^{-/-} mice, respectively, N. Nozaki, K. Helin, T. Kitamura, and K. Nakashima for the anti-Bmi1 antibody (8A9), the anti-Ezh2 antibody (AC22), the pMYS-ires-EGFP vector, and the *Hmga2* cDNA, respectively, and George Wendt for critical reading of the manuscript.

This work was supported in part by Grants-in-aid for Scientific Research (#21390289) and for the Global COE Program (Global Center for Education and Research in Immune System Regulation and Treatment), MEXT, Japan, a Grant-in-aid for Core Research for Evolutional Science and Technology (CREST) from the Japan Science and Technology Corporation (JST), and grants from the Takeda Science Foundation, Astellas Foundation for Research on Metabolic Disorders, and the Tokyo Biochemical Research Foundation. H. Oguro was supported by a postdoctoral fellowship from the Japanese Society for the Promotion of Science.

The authors have no conflicting financial interests.

Submitted: 12 August 2011

Accepted: 27 January 2012

REFERENCES

- Andrieux, J., J.L. Demory, B. Dupriez, S. Quief, I. Plantier, C. Roumier, F. Bauters, J.L. Laï, and J.P. Kerckaert. 2004. Dysregulation and overexpression of HMGA2 in myelofibrosis with myeloid metaplasia. *Genes Chromosomes Cancer*. 39:82–87. <http://dx.doi.org/10.1002/gcc.10297>
- Classen, A.K., B.D. Bunker, K.F. Harvey, T. Vaccari, and D. Bilder. 2009. A tumor suppressor activity of Drosophila Polycomb genes mediated by JAK-STAT signaling. *Nat. Genet.* 41:1150–1155. <http://dx.doi.org/10.1038/ng.445>
- Ema, H., H. Takano, K. Sudo, and H. Nakauchi. 2000. In vitro self-renewal division of hematopoietic stem cells. *J. Exp. Med.* 192:1281–1288. <http://dx.doi.org/10.1084/jem.192.9.1281>
- Ernst, T., A.J. Chase, J. Score, C.E. Hidalgo-Curtis, C. Bryant, A.V. Jones, K. Waghorn, K. Zoi, F.M. Ross, A. Reiter, et al. 2010. Inactivating mutations of the histone methyltransferase gene EZH2 in myeloid disorders. *Nat. Genet.* 42:722–726. <http://dx.doi.org/10.1038/ng.621>
- Fusco, A., and M. Fedele. 2007. Roles of HMGA proteins in cancer. *Nat. Rev. Cancer*. 7:899–910. <http://dx.doi.org/10.1038/nrc2271>
- Guglielmelli, P., R. Zini, C. Bogani, S. Salati, A. Pancrazzi, E. Bianchi, F. Mannelli, S. Ferrari, M.C. Le Bousse-Kerdilès, A. Bosi, et al. 2007. Molecular profiling of CD34⁺ cells in idiopathic myelofibrosis identifies a set of disease-associated genes and reveals the clinical significance of Wilms' tumor gene 1 (WT1). *Stem Cells*. 25:165–173. <http://dx.doi.org/10.1634/stemcells.2006-0351>
- Ikeda, K., P.J. Mason, and M. Bessler. 2011. 3'UTR-truncated Hmga2 cDNA causes MPN-like hematopoiesis by conferring a clonal growth advantage at the level of HSC in mice. *Blood*. 117:5860–5869. <http://dx.doi.org/10.1182/blood-2011-02-334425>
- Iwama, A., H. Oguro, M. Negishi, Y. Kato, Y. Morita, H. Tsukui, H. Ema, T. Kamijo, Y. Katoh-Fukui, H. Koseki, et al. 2004. Enhanced self-renewal of hematopoietic stem cells mediated by the polycomb gene product Bmi-1. *Immunity*. 21:843–851. <http://dx.doi.org/10.1016/j.immuni.2004.11.004>
- Kawamoto, T. 2003. Use of a new adhesive film for the preparation of multipurpose fresh-frozen sections from hard tissues, whole-animals, insects and plants. *Arch. Histol. Cytol.* 66:123–143. <http://dx.doi.org/10.1679/aohc.66.123>
- Konuma, T., H. Oguro, and A. Iwama. 2010. Role of the polycomb group proteins in hematopoietic stem cells. *Dev. Growth Differ.* 52:505–516. <http://dx.doi.org/10.1111/j.1440-169X.2010.01191.x>
- Lessard, J., and G. Sauvageau. 2003. Bmi-1 determines the proliferative capacity of normal and leukaemic stem cells. *Nature*. 423:255–260. <http://dx.doi.org/10.1038/nature01572>
- Lessard, J., A. Schumacher, U. Thorsteinsdottir, M. van Lohuizen, T. Magnuson, and G. Sauvageau. 1999. Functional antagonism of the Polycomb-Group genes *ee* and *Bmi1* in hemopoietic cell proliferation. *Genes Dev.* 13:2691–2703. <http://dx.doi.org/10.1101/gad.13.20.2691>
- Levine, R.L., and D.G. Gilliland. 2008. Myeloproliferative disorders. *Blood*. 112:2190–2198. <http://dx.doi.org/10.1182/blood-2008-03-077966>
- Majewski, I.J., M.E. Blewitt, C.A. de Graaf, E.J. McManus, M. Bahlo, A.A. Hilton, C.D. Hyland, G.K. Smyth, J.E. Corbin, D. Metcalf, et al. 2008. Polycomb repressive complex 2 (PRC2) restricts hematopoietic stem cell activity. *PLoS Biol.* 6:e93. <http://dx.doi.org/10.1371/journal.pbio.0060093>
- Martinez, A.M., B. Schuettengruber, S. Sakr, A. Janic, C. Gonzalez, and G. Cavalli. 2009. Polyhomeotic has a tumor suppressor activity mediated by repression of Notch signaling. *Nat. Genet.* 41:1076–1082. <http://dx.doi.org/10.1038/ng.414>
- Martyré, M.C., N. Romquin, M.C. Le Bousse-Kerdilès, S. Chevillard, B. Benyahia, B. Dupriez, J.L. Demory, and F. Bauters. 1994. Transforming growth factor-beta and megakaryocytes in the pathogenesis of idiopathic myelofibrosis. *Br. J. Haematol.* 88:9–16. <http://dx.doi.org/10.1111/j.1365-2141.1994.tb04970.x>
- Mochizuki-Kashio, M., Y. Mishima, S. Miyagi, M. Negishi, A. Saraya, T. Konuma, J. Shinga, H. Koseki, and A. Iwama. 2011. Dependency on the polycomb protein Ezh2 distinguishes fetal from adult hematopoietic stem cells. *Blood* Oct 31. [Epub ahead of print]. <http://dx.doi.org/10.1182/blood-2011-03-340554>
- Molofsky, A.V., R. Pardal, T. Iwashita, I.K. Park, M.F. Clarke, and S.J. Morrison. 2003. Bmi-1 dependence distinguishes neural stem cell self-renewal from progenitor proliferation. *Nature*. 425:962–967. <http://dx.doi.org/10.1038/nature02060>
- Morin, R.D., N.A. Johnson, T.M. Severson, A.J. Mungall, J. An, R. Goya, J.E. Paul, M. Boyle, B.W. Woolcock, F. Kuchenbauer, et al. 2010. Somatic mutations altering EZH2 (Tyr641) in follicular and diffuse large B-cell lymphomas of germinal-center origin. *Nat. Genet.* 42:181–185. <http://dx.doi.org/10.1038/ng.518>
- Nikoloski, G., S.M. Langemeijer, R.P. Kuiper, R. Knops, M. Massop, E.R. Tönissen, A. van der Heijden, T.N. Scheele, P.Vandenbergh, T. de Witte, et al. 2010. Somatic mutations of the histone methyltransferase gene EZH2 in myelodysplastic syndromes. *Nat. Genet.* 42:665–667. <http://dx.doi.org/10.1038/ng.620>

- Oguro, H., A. Iwama, Y. Morita, T. Kamijo, M. van Lohuizen, and H. Nakauchi. 2006. Differential impact of *Ink4a* and *Arf* on hematopoietic stem cells and their bone marrow microenvironment in Bmi1-deficient mice. *J. Exp. Med.* 203:2247–2253. <http://dx.doi.org/10.1084/jem.20052477>
- Oguro, H., J. Yuan, H. Ichikawa, T. Ikawa, S. Yamazaki, H. Kawamoto, H. Nakauchi, and A. Iwama. 2010. Poised lineage specification in multipotential hematopoietic stem and progenitor cells by the polycomb protein Bmi1. *Cell Stem Cell.* 6:279–286. <http://dx.doi.org/10.1016/j.stem.2010.01.005>
- Park, I.K., D. Qian, M. Kiel, M.W. Becker, M. Pihalja, I.L. Weissman, S.J. Morrison, and M.F. Clarke. 2003. Bmi-1 is required for maintenance of adult self-renewing haematopoietic stem cells. *Nature.* 423:302–305. <http://dx.doi.org/10.1038/nature01587>
- Pietersen, A.M., and M. van Lohuizen. 2008. Stem cell regulation by polycomb repressors: postponing commitment. *Curr. Opin. Cell Biol.* 20:201–207. <http://dx.doi.org/10.1016/j.ceb.2008.01.004>
- Sauvageau, M., and G. Sauvageau. 2010. Polycomb group proteins: multifaceted regulators of somatic stem cells and cancer. *Cell Stem Cell.* 7:299–313. <http://dx.doi.org/10.1016/j.stem.2010.08.002>
- Serrano, M., H. Lee, L. Chin, C. Cordon-Cardo, D. Beach, and R.A. DePinho. 1996. Role of the INK4a locus in tumor suppression and cell mortality. *Cell.* 85:27–37. [http://dx.doi.org/10.1016/S0092-8674\(00\)81079-X](http://dx.doi.org/10.1016/S0092-8674(00)81079-X)
- Simon, J.A., and R.E. Kingston. 2009. Mechanisms of polycomb gene silencing: knowns and unknowns. *Nat. Rev. Mol. Cell Biol.* 10:697–708. <http://dx.doi.org/10.1038/nrm2763>
- Tefferi, A., J. Thiele, A. Orazi, H.M. Kvasnicka, T. Barbui, C.A. Hanson, G. Barosi, S. Verstovsek, G. Birgegard, R. Mesa, et al. 2007. Proposals and rationale for revision of the World Health Organization diagnostic criteria for polycythemia vera, essential thrombocythemia, and primary myelofibrosis: recommendations from an ad hoc international expert panel. *Blood.* 110:1092–1097. <http://dx.doi.org/10.1182/blood-2007-04-083501>
- van der Lugt, N.M., J. Domen, K. Linders, M. van Roon, E. Robanus-Maandag, H. te Riele, M. van der Valk, J. Deschamps, M. Sofroniew, M. van Lohuizen, and A. Berns. 1994. Posterior transformation, neurological abnormalities, and severe hematopoietic defects in mice with a targeted deletion of the bmi-1 proto-oncogene. *Genes Dev.* 8:757–769. <http://dx.doi.org/10.1101/gad.8.7.757>
- Young, A.R., and M. Narita. 2007. Oncogenic HMGA2: short or small? *Genes Dev.* 21:1005–1009. <http://dx.doi.org/10.1101/gad.1554707>
- Yuan, J., M. Takeuchi, M. Negishi, H. Oguro, H. Ichikawa, and A. Iwama. 2011. Bmi1 is essential for leukemic reprogramming of myeloid progenitor cells. *Leukemia.* 25:1335–1343. <http://dx.doi.org/10.1038/leu.2011.85>